Engineering Transactions, **68**(1): 103–114, 2020, doi: 10.24423/EngTrans.1069.20200211
Polish Academy of Sciences • Institute of Fundamental Technological Research (IPPT PAN)
Université de Lorraine • Poznan University of Technology

Research Paper

Lightweighting of Wishbone Finite Element Analysis

Shuxian WANG[1)], Perk Lin CHONG[2)*], David HUGHES[2)]

[1)] *Hubei University of Arts and Science*
School of Automotive and Traffic Engineering
Xiangyang, Hubei 441053, China

[2)] *Teesside University*
School of Computing, Engineering & Digital Technologies
Middlesbrough TS1 3BX, United Kingdom
*Corresponding Author e-mail: p.chong@tees.ac.uk

This paper focuses on lightweighting of wishbone structure for ordinary 5-seated commercial vehicle. Typically, the wishbone structure is made of high carbon steel and the aim is to investigate if the composite materials, such as E-Glass/Epoxy, Carbon/Epoxy and Boron/Epoxy, can achieve the lightweighting purpose without compromising material strength. The study is carried out through finite element package (Siemen NX) with the consideration of three different loading conditions, namely, lateral braking force, vertical and longitudinal braking force. Throughout the study, it is found that both Carbon/Epoxy and Boron/Epoxy composites is able to reduce the weight of the component by 46% while maintaining the required strength.

Key words: Boron/Epoxy; Carbon/Epoxy; E-Glass/Epoxy; finite element analysis; lightweighting; wishbone structure.

1. Introduction

According to the International Energy Agency (IEA), almost one quarter of the global energy production is consumed by transport vehicle [1, 2]. It is proposed that reduction of vehicle weight is one way to reduce the energy consumption and, thus, CO_2 emissions caused by the transport vehicles [3]. The vehicle's weight directly relates to the total fuel consumption [4] that can be reduced up to 35% [5]. The approach is to reduce the weight of product by either reducing the amount of material being used or substituting with lighter material, without compromising the material strength.

Apart from fuel consumption, the stability performance, road handling and comfort of vehicle are key considerations and that depend on the optimum design of suspension system. Of particular interest, the suspension of wishbone struc-

ture is studied in this paper. Vinayak *et al.* implement finite element method to analyse the use of mild steel and aluminium alloy on wishbone structure, the study reveals that the wishbone structure is overdesigned and material removal for weight reduction is proposed [6]. Swapnil *et al.* carries out weight reduction of steel wishbone structure using topological optimisation approach, the weight reduction is observed to be 17.5% [7]. Similar work is done basing on progress meta-model method, which is to optimise 3 shape vectors and 1 thickness with multiple constraints, the finalised weight is reduced by 17.8% [8]. Applying lighter material, i.e. aluminium alloy, for wishbone structure, the weight of the component can be reduced up to 41% by using single constraint optimisation approach [9]. Even though the high amount of weight reduction seems to be promising, it can lead to inefficient geometric design [10] and thus affect manufacturing activities.

Consequently, the trend of lightweighting approach turns to substitute the heavy material by lighter fibre composites, particularly for automotive industry, which can be 50% lighter than steel used whilst maintaining required mechanical properties [11]. It has been claimed that fibre composites is useful for automotive components, where the mechanical, thermal and recycling properties can be improved [12]. The aim of this paper is to investigate the lightweighting effect of wishbone structure for ordinary 5-seated car using fibre composite materials. The approach is carried out through finite element method, which is successfully implemented in automotive field [13, 14].

Paper sections are organised as follows: Section 2 describes the finite element modelling procedures, which details the applied loadings and constraints. Different fibre composites materials are taken into consideration in the modelling process. Section 3 discusses the FEA generated results and compare the effect of using different fibre composites. Section 4 concludes the overall research achievement and propose future research.

2. Finite Element Modelling

The finite element analysis is carried out upon the wishbone structure for 5-seated vehicle, Fig. 1. At the front of the wishbone, there is a ball joint mounting hole connecting to the upright, where the hole encounters load. Whereas, there are two mounting regions to the frame located at the back of the wishbone structure.

The overview of finite element modelling procedures is illustrated in Fig. 2. Initially, the CAD model was input to the Siemen NX software. Subsequently, the finite element mesh was generated, where the idea was as follows: to discretise the CAD model into sufficiently dense meshing to ensure acceptable computational accuracy. The detail about meshing will be presented in Subsec. 2.1.

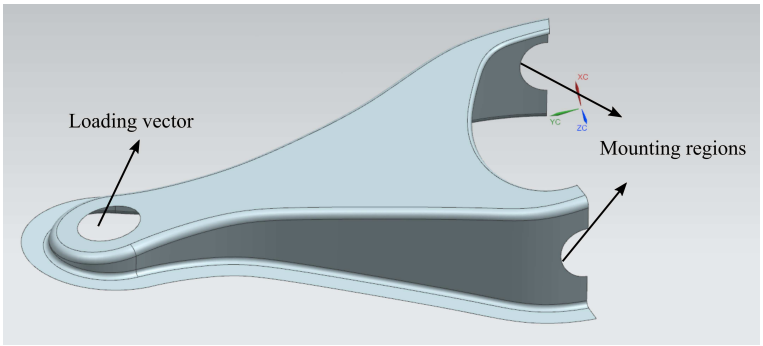

FIG. 1. CAD Model of the Wishbone Structure (© 2019 Siemens Product Lifecycle Management Software Inc.; reprinted with permission).

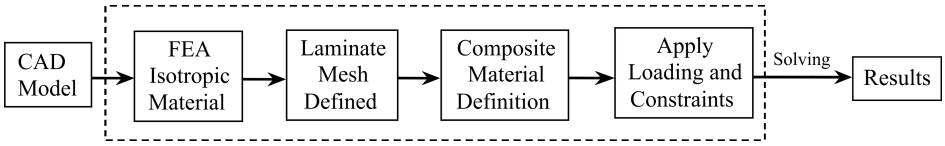

FIG. 2. A scheme for the modelling of the component by means of FEA.

In order to specify the composite material and define the required ply arrangements, an understanding of the stresses distribution under variants of loading is required. An Isotropic FEA material model is defined produced and solved, this highlights principal load paths as illustrated in Fig. 3. The principal load

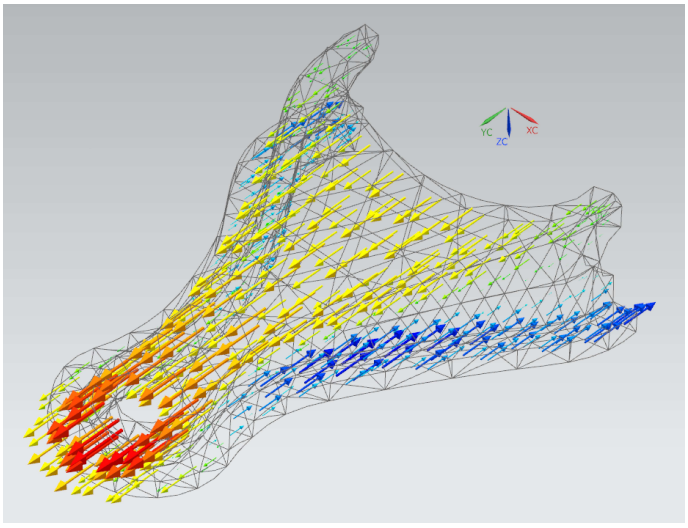

FIG. 3. Wishbone loading (© 2019 Siemens Product Lifecycle Management Software Inc.; reprinted with permission).

paths need to correspond with principal fibre. A global stiffness criterion is also established from the isotropic model by optimising part thickness.

As introduced in Sec. 1, fibre composites are to be evaluated for the wishbone structure. For the analysis full anisotropic material properties, such as number of stacking layers, fibre directions and mechanical parameters need to be provided. The details are given in Subsec. 2.2.

After the material properties are defined, the load is applied at the hole as shown in Fig. 1. Three loading cases will be taken into consideration, which includes vertical load, lateral load and braking load. The constraints are applied at the back of the wishbone. The details will be described in Subsec. 2.3.

Once the information of mesh, material properties, applied load and constraints are provided, the finite element model can then be solved based on linear static analysis. The outputs are the results of stress and displacement distributions. The results will be discussed in Sec. 3.

2.1. Meshing

The 2-D thin shell quadrilateral element is implemented (Fig. 4a), it is useful for modelling arbitrary shape of curved shell geometries as of the wishbone

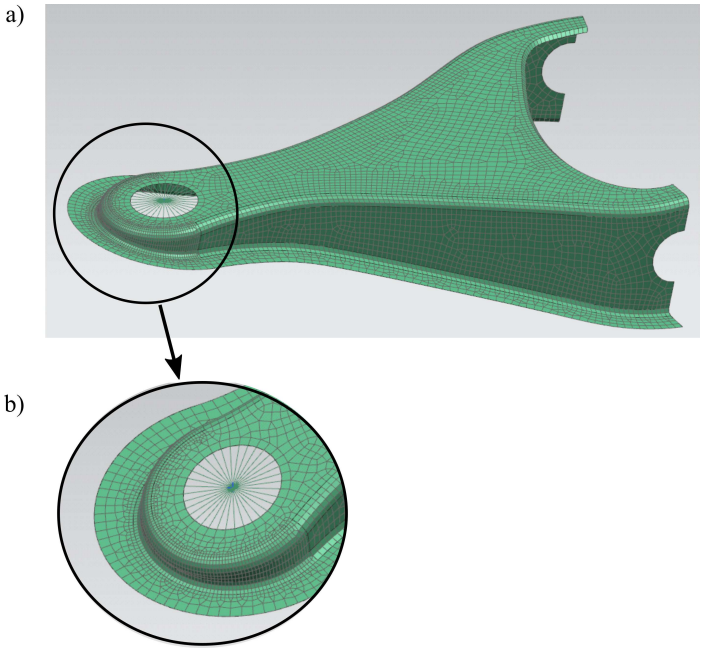

Fig. 4. (a) Meshing of wishbone structure; (b) 1-D connector within the front hole of wishbone structure ().

structure [15]. It is noted that there are 7525 elements with the size of 4 mm being used to approximate the shape of wishbone structure. In the case of 2-D element, the related thickness is required to be defined.

It is noted that there should be a bolted joint at the front hole of the wishbone structure, which is to connect to the wheel. It is reasonable to model the bolted joint as a point of loading within the front hole. The element of 1-D connector is defined within the front hole as shown in Fig. 4b.

2.2. Defining material

It is demonstrated in section 1 that fibre composite materials are effectively used for lightweigthing of automotive components. The global stiffness analysis described in 2.0 and previous data has identified, E-Glass/Epoxy, Carbon/Expoxy and Boron Epoxy as appropriate for the application. These materials have previously been used for automotive drive shafts [16, 17]. These 3 composite materials are therefore to be evaluated for the wishbone structure, and the respective material properties [16, 17] are given in Table 1. The allowable stress is defined as maximum tensile strength. This parameter is taken for evaluating the stress level from FEA.

Table 1. Properties of E-Glass/Epoxy, Carbon/Epoxy and Boron/Epoxy.

Property	E-glass/Epoxy	Carbon/Epoxy	Boron/Epoxy
E_{11} [GPa]	50	126.9	204
E_{22} [GPa]	12	11	18.5
G_{12} [GPa]	5.6	6.6	5.59
ν_{12}	0.3	0.3	0.3
Allowable stress [MPa]	400	440	630
ρ [kg/m^3]	2000	1600	2000
V_f	0.6	0.6	0.6

Based on the analysis described in 2.0 laminate thickness and loading distributions are established. Ply layup is standardised for the three materials evaluated. An orthotropic ply layup is developed with fibres laid in three different principal axes [0, 90, 45°]. The composite laminates are built from 25 layers of woven plies (PPG-PL-3K). The stacking sequence is [90/0/−45/45/90] as shown in Fig. 5. Carbon/Epoxy, Eglass/Epoxy and Boron/Epoxy are operated in the similar manner. The number of plies is studied in relation to the lightweighting effect and material deformation.

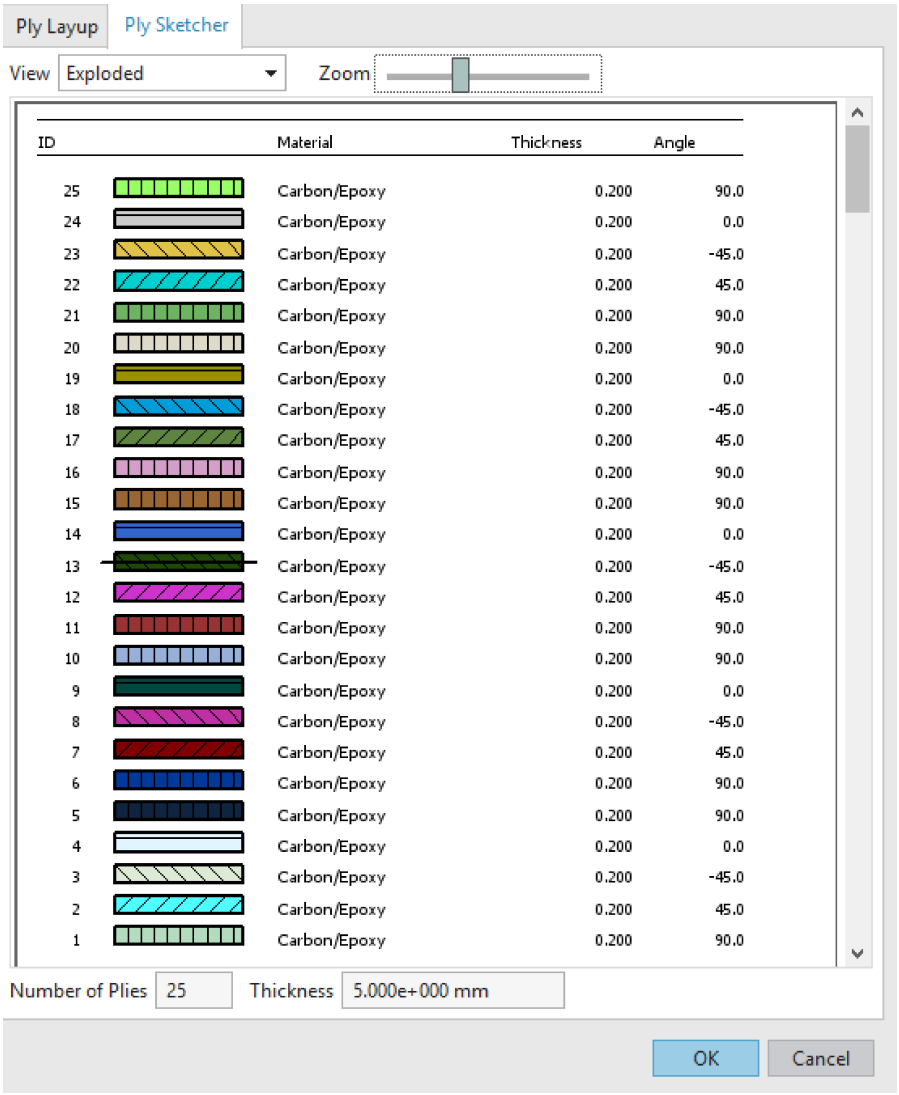

FIG. 5. Information of laminate stacking (© 2019 Siemens Product Lifecycle Management Software Inc.; reprinted with permission).

2.3. Loading and constraints

In general, the force scheme of automobile suspension system can be considered as brake impact. For braking condition, the wishbone structure is subjected to longitudinal force F_y, Fig. 6. In the case of vertical vibration condition, the wishbone structure is loaded by vertical force F_z, Fig. 7. The wishbone structure under lateral force F_x, Fig. 8. The forces are estimated as $F_y = 2000$ N, $F_z = 5100$ N, and $F_x = 5300$ N [18]. To model the motion, the back of the

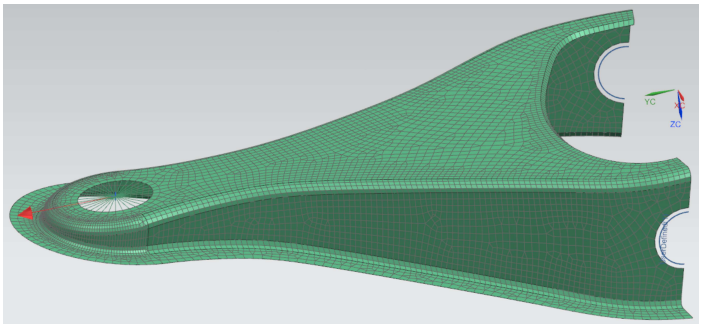

FIG. 6. Braking force applied on the wishbone structure (© 2019 Siemens Product Lifecycle Management Software Inc.; reprinted with permission).

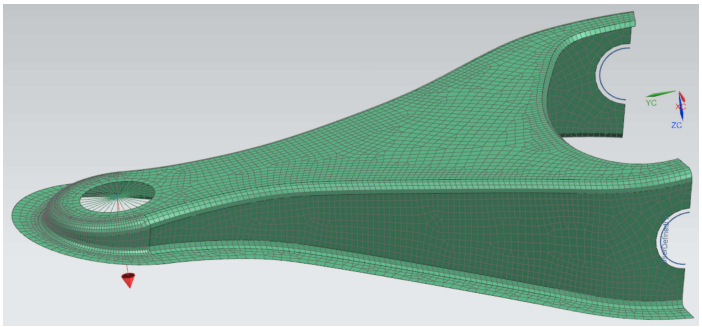

FIG. 7. Vertical force applied on the wishbone structure (© 2019 Siemens Product Lifecycle Management Software Inc.; reprinted with permission).

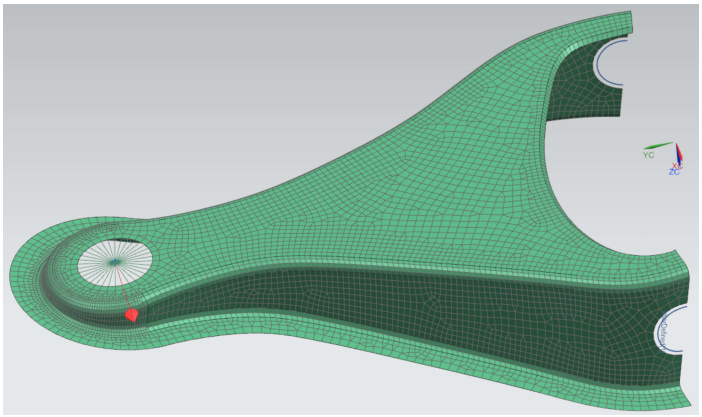

FIG. 8. Lateral force applied on the wishbone structure (© 2019 Siemens Product Lifecycle Management Software Inc.; reprinted with permission).

wishbone structure only allows rotation along x-axis, and fix the remaining of rotational and translational motions.

3. Results discussion

Considering the case of AISI 1095 Carbon Steel for the wishbone structure, the yield stress is 525 MPa and the mass takes 2.2 kg. Figure 9a illustrates the stress distribution on the wishbone structure under braking force of $F_y = 2000$ N. At the upper face of the component, the stress exerted at the edge is about 31.8 MPa and the stress reduced towards inner part to the level of 7.96 MPa, Fig. 9a, it demonstrates the stretching of the wishbone structure. The maximum stress of 95.48 MPa occurs at the mounting zones. Figure 9b shows the stress distribution due to the vertical force of $F_z = 5100$ N, which generates bending effect of the wishbone structure, where the stress on upper face is gradually increased from stress level of 27.34 MPa to 109.34 MPa. The maximum stress of 328.02 MPa appears at the mounting position. Figure 9c demonstrates the stress distribution subject to lateral force of $F_x = 5300$ N. This result exhibits twisting effect at upper surface and the stress gradually increase from inner to outer

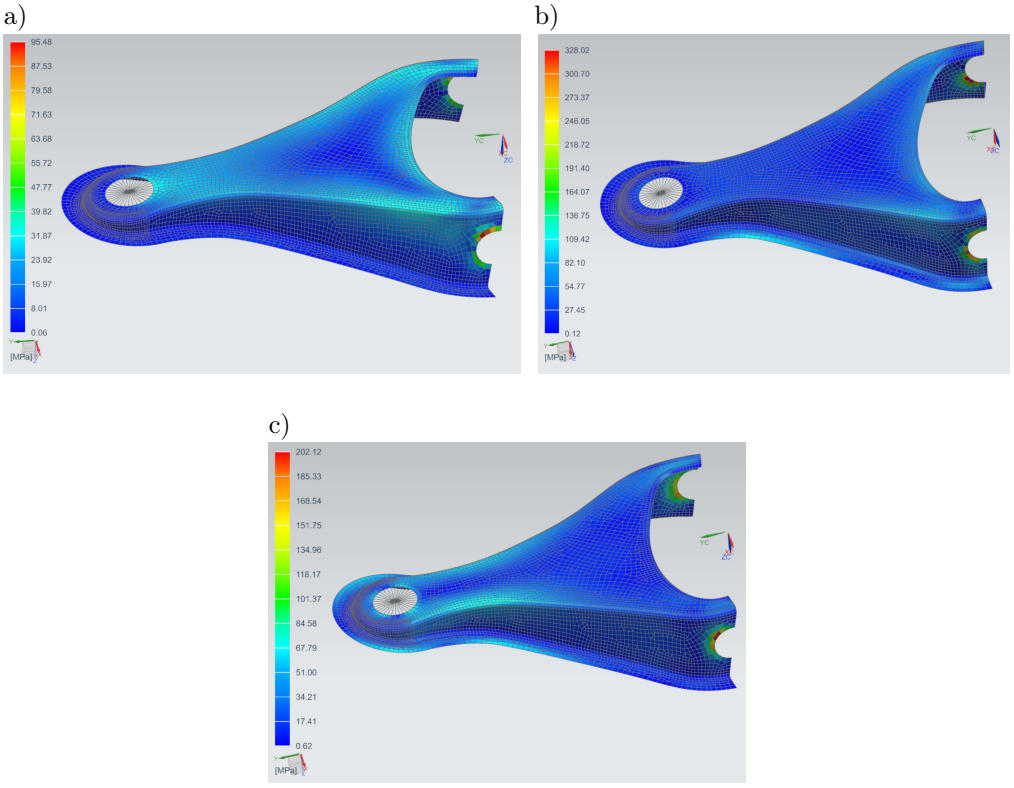

Fig. 9. Stress distribution of wishbone structure under: a) braking force F_y, b) vertical force F_z, c) lateral force F_x (© 2019 Siemens Product Lifecycle Management Software Inc.; reprinted with permission).

part ranging from 16.84 MPa to 67.37 MPa. Similar to the braking and vertical loading conditions, the maximum stress occurs at mounting regions reaching 202.12 MPa.

The maximum stresses as mentioned above is far lower than the allowable stress limit of 525 MPa. This indicates that there is a likelihood to lighten the wishbone structure.

Considering that the AISI 1095 Carbon Steel is replaced by lighter composite material, namely, E-Glass/Epoxy, Carbon/Epoxy and Boron Epoxy values of the maximum stress are considered as a function of the wishbone thickness at the resulted mass, Fig. 10.

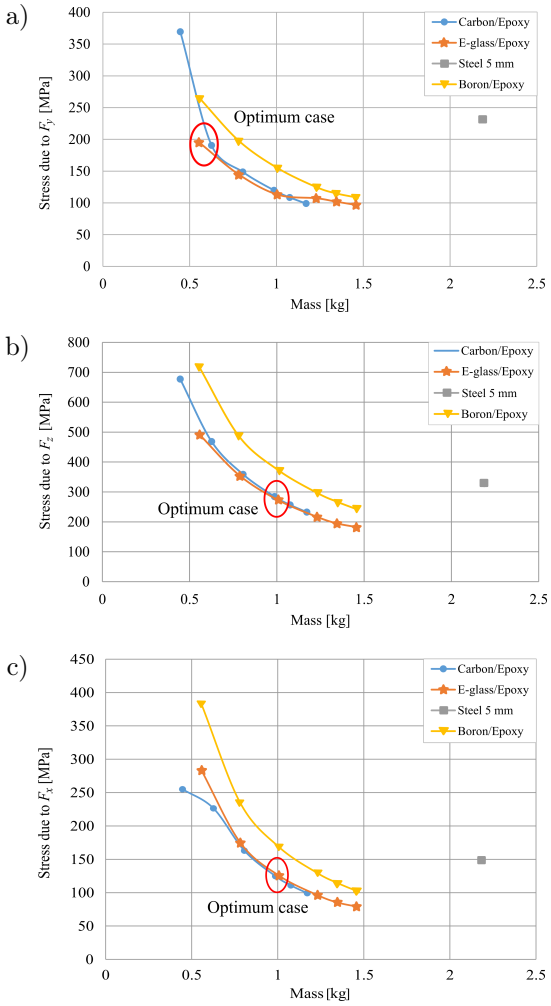

FIG. 10. Variation of maximum stress with respect to mass for different materials under: a) braking force F_y, b) vertical force F_z, c) lateral force F_x.

Figure 10a illustrates the variation of mass with respects to maximum stress when it is under braking force of $F_y = 2000$ N. As a matter of practical convenience, the simulation exercise is carried out by incremental thickness from 5 mm, 7 mm, 9 mm, 11 mm, 12 mm, and 13 mm of the wishbone structure with a defined composite material. Looking on the variation of stress of Carbon/Epoxy, starting with 5 mm thickness, the respective mass is approximately 0.45 kg and the maximum stress is of 370 MPa. Compare to the 5 mm thickness of steel (corresponding mass of 2.2 kg), the maximum stress of 150 MPa is much lower. This encourages to increase the thickness to 6 mm, correspondingly, the mass is increased reaching 0.63 kg and the respective maximum stress drops significantly obtaining 190 MPa. When the thickness takes 13 mm (corresponding mass of 1.2 kg), the maximum stress drops to 100 MPa. This demonstrates that the maximum stress is much lower than when the material is defined as steel, and the mass can be reduced by 45%. The E-glass epoxy and Boron epoxy have similar variations as shown in Fig. 10a, and the corresponding maximum stresses of 97 MPa and 110 MPa. The respective masses for both defined materials are 1.46 kg, and the mass reduction is of 34%. The finalised masses for all materials have reduced significantly, however, the respective thicknesses of 13 mm are not practically appropriate. Considering the mass, thickness and maximum stress level, the optimum point is E-glass epoxy at 0.6 kg, Fig. 10a, such that the mass reduction is of 73%.

Figures 10b and 10c illustrate the variations of the maximum stress as a function of the thickness and the mass obtained when it is under vertical force of $F_z = 5100$ N and lateral force of $F_x = 5100$ N. Both of the variation patterns are similar to that when the wishbone structure is under braking force of $F_y = 2000$ N. When looking in to the loading conditions for vertical force (see Fig. 10b) and lateral force (see Fig. 10c), the maximum stresses for Boron/Epoxy is the highest and thus it is not favourable. For vertical force condition, the optimum point occurs at 1 kg of Carbon/Epoxy, and the corresponding maximum stress is of 275 MPa, Fig. 10b. Similar to vertical force condition, the optimum point for lateral force condition occurs at 1 kg of Carbon/Epoxy, and the corresponding maximum stress is of 110 MPa as shown in Fig. 10c. Consequently, the optimum choice is of 1 kg of Carbon/Epoxy, where the maximum stress level lower than that of steel in all the 3 different loading conditions. The finalised mass reduction is of 54.5%.

4. Conclusions

The investigation on lightweighting the wishbone structure by using composite materials was carried out. The effectiveness of composite materials, namely, Carbon/Epoxy, Eglass/Epoxy and Boron/Epoxy was assessed based on various

loading conditions using finite element analysis. It was found that Carbon/Epoxy is the most optimal choice, where the mass is 54.5% lower than that the original material of AISI 1095 Carbon Steel. The maximum stress was noticed for the vertical force F_z reaching 275 MPa. All the stresses are within the allowable stress limit of 440 MPa. In the case of the composite considered the maximum values of stress were lower than that the ones in the AISI 1095 Carbon Steel.

Acknowledgement

The research was mainly supported by Teesside University and Open fund of Hubei Superior and Distinctive Discipline Group of "Mechatronics and Automobiles". The authors would also like to acknowledge the anonymous reviewers who played a significant role in shaping and improving the manuscript.

References

1. *IEA: Energy statistics of non-OECD countries*, International Energy Agency, Paris, 2003.
2. *IEA: Energy statics of OECD countries.* International Energy Agency, Paris, 2003.
3. Helms H., Lambrecht U., The potential contribution of light-weighting to reduce transport energy consumption, *International Journal of Life Cycle Assessment*, **12**(1): 58–64, 2007, doi: 10.1065/lca2006.07.258.
4. Koffler, C., Rodhe-Branderburger K., On the calculation of fuel savings through lightweight design in automotive life cycle assessments, *International Journal of Life Cycle Assessment*, **15**(1): 128–135, 2010, doi: 10.1007/s11367-009-0127-z.
5. Cheah L., Evans C., Bandivadekar A., Heywood J., Factor of two: halving the fuel consumption of new US automobiles by 2035, [in:] *Reducing Climate Impacts in the Transportation Sector*, Cannon J.S., Sperling D. [Eds], pp. 49–71, 2008.
6. Kulkarni V., Jadhav A., Basker P., Finite element analysis and topology optimization of lower arm of double wishbone suspension using RADIOSS and optistruct, *International Journal of Science and Research*, **3**(5): 639–643, 2014.
7. Swapnil S.K., Amol N.P., Amol B.G., Design optimisation of a lower control arm of suspension system in a LCV by using topological approach, *International Journal of Innovative Research in Science, Engineering and Technology*, **6**(6): 11657–11665, 2017, doi: 10.15680/IJIRSET.2017.0606084.
8. Heo S.J., Kang D.O., Lee J.H., Kim I.H., Darwish S.M., Shape optimization of lower control arm considering multi-disciplinary constraint condition by using progress meta-model method, *International Journal of Automotive Technology*, **14**(3): 499–505, 2013, doi: 10.1007/s12239-013-0054-7.
9. Viqaruddin M., Reddy D.R., Structural optimization of control arm for weight reduction and improved performance, *Materials Today: Proceedings*, **4**(8): 9230–9236, 2017, doi: 10.1016/j.matpr.2017.07.282.

10. Yildiz A.R., Kaya N., Ozturk F., Alankus O., Optimal design of vehicle components using topology design and optimisation, *International Journal of Vehicle Design*, **34**(4): 387–398, 2004, doi: 10.1504/IJVD.2004.004064.

11. Wilson A., Vehicle weight is the key driver for automotive composites, *Reinforced Plastics*, **61**(2): 100–102, 2017, doi: 10.1016/j.repl.2015.10.002.

12. Jeyanthi S, Rani J.J., Influence of natural long fiber in mechanical, thermal and recycling properties of thermoplastic composites in automotive components, *International Journal of Physical Sciences*, **7**(43): 5765–5771, 2012, doi: 10.5897/IJPS12.521.

13. Setiawan R., Salim M.R., Crashworthiness design for an electric city car against side pole impact, *Journal of Engineering and Technological Sciences*, **49**(5): 587–603, 2017, doi: 10.5614/j.eng.technol.sci.2017.49.5.3.

14. Wicaksono S., Rahman MR., Mihradi S., Prifiharni S., Finite element analysis of bus rollover test in accordance with UN ECE R66 Standard, *Journal of Engineering and Technological Sciences*, **49**(6): 799–810, 2017, doi: 10.5614/j.eng.technol.sci.2017.49.6.7.

15. Katili I., Maknun I.J., Batoz J.L., Ibrahimbegovic A., Shear deformable shell element DKMQ24 for composite structures, *Composite Structures*, **202**: 182–200, 2018, doi: 10.1016/j.compstruct.2018.01.043.

16. Rangaswamy T., Vijayrangan S., Optimal sizing and stacking sequence of composite drive shafts, *Materials science*, **11**(2): 133–139, 2005.

17. Reddy P.S., Nagaraju C., Weight optimization and finite element analysis of composite automotive drive shaft for maximum stiffness, *Materials Today: Proceedings*, **4**(2, A): 2390–2396, 2017, doi: 10.1016/j.matpr.2017.02.088.

18. Song Z., Zhao X., Research on lightweight design of automobile lower arm based on carbon fiber materials, *World Journal of Engineering and Technology*, **5**(4): 730–742, 2017, doi: 10.4236/wjet.2017.54061.

Received June 12, 2019; accepted version December 16, 2019.
